# Wide, Continuously Swept VCSEL Using a Novel Air-Cavity-Dominant Design

**Pengfei Qiao[1], Kevin T. Cook[1], Jipeng Qi[1], Larry A. Coldren[2] and Connie J. Chang-Hasnain[1]**
*1: EECS Department and Tsinghua-Berkeley Shenzhen Institute, University of California, Berkeley, CA 94720, USA*
*2: Department of Electrical and Computer Engineering, University of California, Santa Barbara, CA 93117, USA*
*Email address: cch@berkeley.edu*

**Abstract:** We report electrically-pumped MEMS-VCSELs with a record 70 nm continuous wavelength sweep at 1057-nm with 600 kHz rate using a novel air-cavity-dominant design. Such devices are promising for swept-source OCT and 3D sensing applications. 
**OCIS codes:** (140.7260) Vertical cavity surface emitting lasers; (050.6624) Subwavelength structures; (230.4685) Optical microelectromechanical devices; (260.2110) Electromagnetic optics; (140.3600) Lasers, tunable.

## 1. Introduction

Wavelength-tunable lasers are important for many applications including optical fiber communications, optical coherence tomography (OCT), light detection and ranging (LIDAR), and high resolution laser spectroscopy. Vertical-cavity surface-emitting lasers (VCSELs) have exhibited advantages over edge-emitting lasers including lower cost, smaller footprint, and lower power consumption [1]. Using a microelectromechanical system (MEMS), one can vary the optical cavity length of a VCSEL and continuously tune/sweep the lasing wavelength without hops or hysteresis. Since the first MEMS-tunable VCSEL was reported in 1995 [2], many advances have been reported for center wavelengths at 850, 940, 980, 1060, 1310 and 1550 nm [3]. The 1060 nm tunable VCSELs are of interests for applications in short-wavelength division multiplexed (SWDM) fiber communications and swept-source OCT systems for ophthalmic and fiber endoscopic imaging. In an OCT, the axial resolution is inversely proportional to the tuning ratio (tuning range divided by center wavelength or $\Delta\lambda/\lambda_0$) and the field of view is proportional to the sweep rate. Hence, both continuously tuning ratio and sweep rate are important for these applications.

Previously a very wide tuning range for an electrically-pumped VCSEL was demonstrated at 1550 nm with 102 nm range (tuning ratio $\Delta\lambda/\lambda_0$ is 6.58%) but at a relatively slow speed of 215 Hz due to electrothermally tuning mechanism [4]. John et al. published a $\Delta\lambda/\lambda_o$=6.1% tuning ratio (63.8 nm) centered at 1046 nm with a 240 kHz sweep-rate [5]. Recently, we reported a new design leading to a record tuning ratio of 6.9% (73 nm) at the center wavelength of 1060 nm [3]. In that paper we introduced the concept of an air-cavity-dominant design with relatively low optical intensity in the semiconductor cavity at the center wavelength. Here, we explain with a clear model how this design works. Further, we demonstrate a dynamic tuning of 6.6% (70 nm) with a fast speed of 600 kHz, a record value for an electrically pumped VCSEL, to the best of our knowledge.

## 2. VCSEL Design

The schematic and the scanning electron microscopy (SEM) image of our 1060-nm MEMS tunable VCSEL are shown in FIG. 1. The device consists of a semiconductor portion, a top high-contrast grating (HCG) mirror, and an air gap in between forming an air cavity. An HCG is a single layer of high refractive index material with near-wavelength dimensions. They have shown to exhibit high reflectivity across a wide range of wavelengths [3], replacing traditional distributed Bragg reflectors (DBR) as top mirror for a VCSEL. The HCGs are lightweight and excellent for high speed wavelength tuning, and can be produced by simple fabrication methods with high tolerance.

The semiconductor portion (starting from the top) includes a semiconductor-air coupling (SAC) region, a couple of pairs of p-DBRs (with $Al_{0.9}Ga_{0.1}As$ low-index layer first, followed by high-index $Al_{0.12}Ga_{0.88}As$ layer), a quarter-lambda $Al_{0.98}Ga_{0.02}As$ layer for oxidation, a lambda-thick cavity with three quantum wells in the center, followed by 38.5 pairs of n-DBRs, all grown on a n-doped GaAs substrate. The SAC region consists of a few layers, collectively designed to control the coupling between the semiconductor and air cavities. The SAC region comprises, listed from the top, an InGaP etch stop, a GaAs contact, and a graded $Al_xGa_{1-x}As$ layer, all of which combine to be the half-lambda window layer. The air gap is formed by selectively remove the GaAs sacrificial layer by selective wet etching. The fabrication process is similar to our 1060-nm SCD VCSELs in [3].

Conventional MEMS-tunable VCSELs have high reflection at the semiconductor-air interface and the optical field penetration into air is suppressed, referred as the semiconductor-cavity dominant (SCD) design. To extend the tuning range, researchers have applied a quarter-lambda thick anti-reflection (AR) layer with refractive index close to the geometric mean of the semiconductor refractive index and the refractive index of air. This configuration was

referred to as the extended-cavity (EC) design. In that case, the semiconductor and air cavities are perfectly matched. They resonate as one cavity, as if the original semiconductor cavity "extends" into the air region. Designs in [4, 5] belong to the EC case. The air-cavity-dominant (ACD) design is a case in which the semiconductor-air reflection is designed to be out of phase with the semiconductor cavity, causing the optical field to be confined more significantly in the air cavity at the center wavelength.

## 3. Semiconductor-Air Cavity Coupling

FIG. 2 shows the transfer-matrix calculated resonance wavelengths as functions of the air gap thickness for four longitudinal Fabry-Perot (FP) modes. The dominant lasing mode is determined by lowest threshold gain among all FP modes, as indicated by the green circled lines in FIG. 2, for SCD, EC, and ACD designs. From the cold-cavity simulation we observe significant improvement of the tuning range from 59 nm (SCD), to 79 nm (EC), and to 96 nm (ACD). Note the tuning range is limited by FP mode spacing (free spectra range FSR) at the tuning edges. The gray areas in FIG. 2 indicate the reflectivity of the hybrid top mirror is below 99.5%, hence unlikely to support lasing. The three configurations exhibit distinct shapes of their tuning curves, namely a mirrored S-shape for SCD, a straight line for EC, and an S-shape for ACD. The threshold material gain was calculated using transmission matrix method [6] for all three configurations. We find that the threshold material gain for ACD is only 6% higher than SCD at the tuning center.

We perform the finite-difference time-domain simulation of the field spectra at sampled observation points in the semiconductor cavity as a function of air gap thickness for SCD, EC and ACD (Fig. 3). The contour spectra confirm the shapes of the tuning curves in Fig. 2. Here we can identify two sets of asymptotic lines for each design. One can already conjecture that these are resonance lines dominated by the semiconductor and air cavities. Using the FP condition of the air cavity sandwiched between two effective mirrors, the wavelength tuning relation is derived as

$$\lambda_r(d) = \frac{2}{m}\left(d + L_{eff}\right) \qquad (1)$$

where d is the air gap thickness, *m* is the FP mode number, and the tuning slope is $\Delta\lambda_r/\Delta d = 2/m$. The blue and purple dashed lines in FIG. 3 correspond to semiconductor- and air-dominant resonances, respectively. For SCD, the purple and blue resonance lines are fitted with $L_{eff}$=31.8 and 0.6 μm, respectively. For EC, the purple and blues lines are fitted with $L_{eff}$=9.7 and 3.2 μm, respectively. Finally with ACD, it should be noted that the resonance lines reside on the blue lines instead of the purple lines. The fitting of purple and blue lines are $L_{eff}$ =13.0 and 3.2 μm, respectively, with all lengths assumed to be in air. Since the $L_{eff}$ varies significantly, it is critical to understand the physical reasons.

We turned to the traditional method to determine the effective length in a multi-layer medium by taking derivative of reflection phase with wavelength [6] for the air and semiconductor cavities for each design. The effective cavity length looking from the center of the air cavity is thus

$$L_{eff} = -\frac{\lambda^2}{4\pi}\frac{d}{d\lambda}\left(\phi_{HCG}(\lambda) + \phi_s(\lambda)\right)\Big|_{\lambda=\lambda_r} \qquad (2)$$

Where $\phi_{HCG}(\lambda)$ and $\phi_s(\lambda)$ are reflective phase for an HCG and the entire epitaxial structure below air gap. The penetration depth at the tuning center resonance of $\lambda_r$=1060 nm for HCG is 0.48 μm and relatively independent of wavelength. The effective length for the below-air region of SCD, EC, and ACD are sensitive to wavelength. The $L_{eff}$ for SCD at the center and edge of tuning range are 32.1 and 1.8 μm, respectively. The $L_{eff}$ for EC at the center and edge of tuning range are 9.7 μm, and 5.2 μm at the tuning center, respectively. The $L_{eff}$ for ACD at the center and edge of tuning range are 3.2 and 12.6 μm, respectively. These values agree well with the asymptotic $L_{eff}$ values obtained from Eq(1) for blue and purple lines, and hence explained the effect of the SAC region in creating different $L_{eff}(\lambda)$, which in turn limits the FSR and thus the tuning range. Further, for ACD, both the value and change are much less with 3.2 μm at the center and 12.6 μm at the edge, resulting a larger FSR over a wide wavelength range.

## 4. Experimental Results

Previously, with a combination of thermal, current and electrostatic tuning, a single-mode continuous lasing across a 73-nm range was demonstrated in [3]. In this paper, with an optimized MEMS design, we obtain a continuous sweep with a DC tuning voltage of 30.2 V plus an AC tuning voltage of 5.2 V at 600 kHz sweep rate, as shown in FIG. 5. The full dynamic tuning range is 69.7 nm, spanning from 1022.5 nm to 1092.2 nm, which is a direct proof of the extended FSR by our ACD design, and is close to calculated tuning range of around 76 nm, showing the tuning range is FSR-limited instead of threshold-limited.

In summary, we demonstrated electrically pumped VCSELs with an ultrahigh tuning ratio of 6.6% using our novel ACD configuration. We investigate in-depth the mechanism of such large improvement over conventional and

AR-coated tunable VCSELs. The wavelength tuning characteristics reside on air-cavity dominant resonance lines, resulting in smaller effective cavity length. Our measurements of the ACD devices confirm our theory of the tuning ratio with MEMS resonance tuning at a fast speed of 600 kHz.

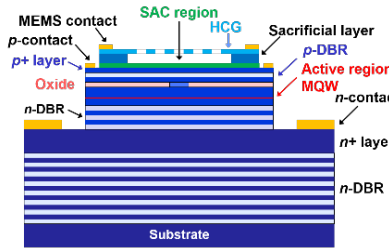


Figure. 1. Schematic of a MEMS-HCG tunable VCSEL with an engineered semiconductor-air coupling (SAC) region.

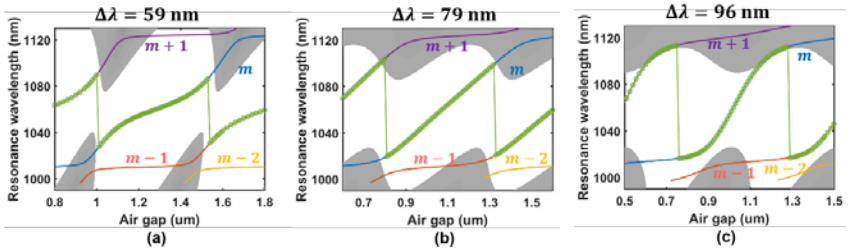


Figure. 2. Resonance wavelengths versus air gap thicknesses for m+1, m, m-1, and m-2 longitudinal modes shown in purple, blue, red, and orange, respectively, for (a) SCD, (b) EC, and (c) ACD designs. The dominant resonance modes, determined by the lowest threshold gain, are shown as green circled lines, indicating tuning ranges of 59 nm, 79 nm, and 96 nm for SCD, EC, and ACD designs, respectively. Zero pairs of top DBR and 38.5 pairs of bottom DBRs are used. Shaded areas indicate hybrid top mirror reflectivity below 99.5%.

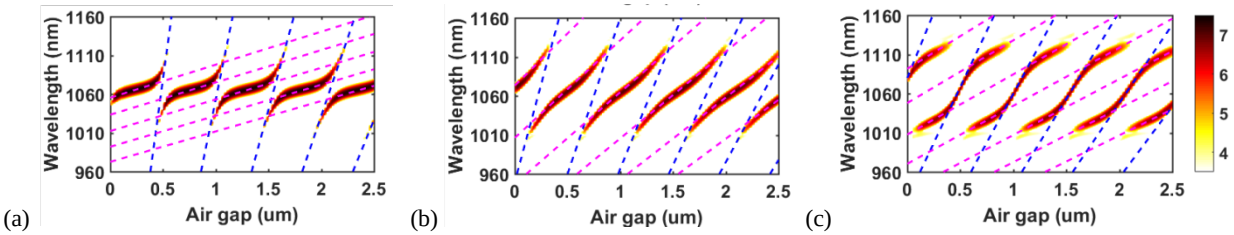


Figure. 3. FDTD-simulated field spectra (log scale) as functions of the air gap thickness d using the (a) SCD, (b) EC, and (c) ACD designs. The high field intensities indicate the resonant wavelength for a given air gap value. Two pairs of top DBR and 38.5 pairs of bottom DBRs are used. The extracted tuning ranges are (a) 41 nm, (b) 59 nm, and (c) 76 nm. The blue and purple dashed lines are the air-dominant and semiconductor-dominant resonance lines, respectively.

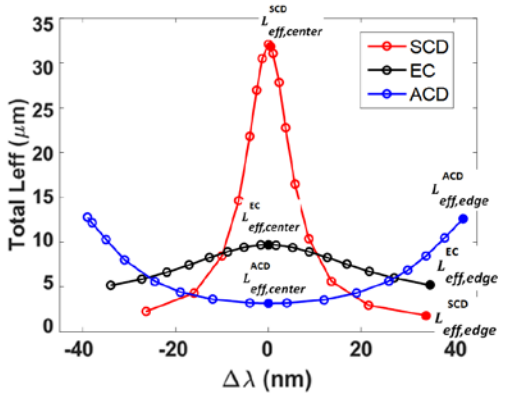


Figure.4. Total effective length calculation as a function of resonance wavelength for SCD, EC, and ACD designs looking from the center the airgap cavity, and again using effective lengths in air.

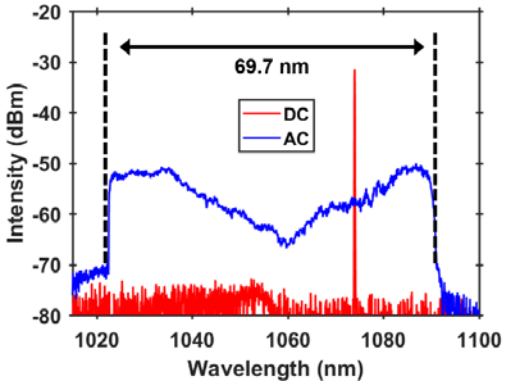


Figure. 2. Measured swept VCSEL spectra for an ACD tunable VCSEL at 6 mA current injection under a constant DC bias (red) and with an additional 600 kHz AC (blue) tuning voltage.

## References

[1] F. Koyama, "Recent advances of VCSEL photonics," IEEE J. Lightwave Technol., vol. 24, no. 12, pp. 4502-4513, 2006.
[2] M. S. Wu, E. C. Vail, G. S. Li, W. Yuen and C. J. Chang-Hasnain, "Tunable micromachined vertical cavity surface emitting laser," Electron. Lett., vol. 31, no. 19, pp. 1671-1672, 1995.
[3] P. Qiao, K. T. Cook, K. Li, and C. J. Chang-Hasnain, "Wavelength swept VCSELs," IEEE J. Sel. Top. Quantum Electron., vol. 23, no. 6, 1700516, 2017.
[4] C. Gierl, T. Gruendl, P. Debernardi, K. Zogal, C. Grasse, H. A. Davani, G. Böhm, S. Jatta, F. Küppers, P. Meißner, and M.-C. Amann, "Surface micromachined tunable 1.55 μm-VCSEL with 102 nm continuous single-mode tuning," Opt. Express, vol. 19, no. 18, pp. 17336-17343, 2011.
[5] D. D. John, C. B. Burgner, B. Potsaid, M. E. Roberson, B. K. Lee, W. J. Choi, A. E. Cable, J. G. Fujimoto and V. Jayaraman, "Wideband electrically pumped 1050-nm MEMS-tunable VCSEL for opthalmic imaging," J. Lightwave Technol., vol. 33, no. 16, p. 3461, 2015.
[6] Larry Coldren, Scott Corzine, and Milan Mašanović , *Diode Lasers and Photonic Integrated Circuits*, J. Wiley, New York, New York 2012.